

**Extreme shock effects in relatively enriched shergottite Northwest Africa 4797.** Walton E. L.<sup>1\*</sup>, Irving A. J.<sup>2</sup>, Bunch T. E.<sup>3</sup>, Kuehner S. M.<sup>2</sup> and Herd C. D. K.<sup>1</sup> <sup>1</sup>Dept. of Earth & Atmospheric Sciences, University of Alberta, Edmonton, AB, T6G 2E3, Canada, <sup>2</sup>Dept. of Earth & Space Sciences, University of Washington, Seattle, WA 98195, <sup>3</sup>Dept. of Geology, Northern Arizona University, Flagstaff, AZ 86011. \*email: [ewalton@ualberta.ca](mailto:ewalton@ualberta.ca)

**Introduction:** All Martian meteorites have been ejected from Martian near-surface regions by impact events capable of accelerating material  $\geq 5$  km/s. The extreme physical conditions of impact, or ‘shock’, cause significant changes in the texture, mineralogy and isotopic composition of the rocks [1, 2]. Every Martian meteorite records some features associated with shock, with variable intensity, ranging from the least shocked nakhlites to the most strongly shocked shergottites [2]. The general convention has been to ascribe all shock features to impact ejection from Mars, with the exception of ALH 84001 and NWA 2737 [3, 4]; however, a recent study on shergottite Dhofar 378 (55–75 GPa; [5]), has shown that an Ar-Ar age of  $\sim 141$  Ma most likely dates a major impact on Mars, with later ejection at 3 Ma in a smaller impact event. This suggestion raises the question whether the shock features observed in other shergottites were formed at the time of Mars ejection or earlier in Martian history. This is particularly true for highly shocked samples where the complex textures can lead to debate over the details of these processes, in particular on the number of shock events required to explain observed textures.

This study reports new data on strongly shocked shergottite Northwest Africa (NWA) 4797, found in 2001 near Missouri, Morocco as a single stone weighing 15.0 grams [6]. A total of 3.3 g was made available for study. Here, we focus on detailed analysis of shock metamorphic effects in NWA 4797 in order to constrain the equilibration shock pressure.

**Petrography:** Microtextures were characterized using BSE and SE images using a JEOL 6301F Field Emission SEM with an 8 mm working distance and an accelerating voltage of 20 kV. Mineral modes for the thin section were determined by manual point counting on BSE images ( $n = 12,000$ ).

*Igneous Lithologies and Oxygen Fugacity.* NWA 4797 exhibits two igneous lithologies – poikilitic and non-poikilitic. The stone is composed principally of mm-size grains of olivine (40.3%), pyroxene (33.9%), and smaller (80 – 450  $\mu\text{m}$ ) regions of interstitial glass or recrystallized glass (after plagioclase; 9.1%). Minor phases include chromite (3.5%), merrillite (0.8%), and melt inclusions (0.4%). The sample is highly vesiculated (1.6%). Pyroxene abundances have been further refined using elemental X-ray maps; the modal abundances of pigeonite and augite are 22.1% and 11.8%, respectively.

Compositions of the earliest formed pyroxene, olivine and chromite yield  $f\text{O}_2 = 0.8$  log units above the Iron-Wüstite (IW) buffer (FMQ – 2.5), following the method of [7]. This result is within error of estimates for “lherzolitic” shergottites such as ALH 77005 [8]. A relative increase in  $f\text{O}_2$  during crystallization is indicated from spinel-ilmenite pairs in the non-poikilitic areas, which yield  $f\text{O}_2 \sim \text{IW} + 3$  (FMQ – 0.5).

*Shock metamorphism:* NWA 4797 is texturally complex, with strong shock overprinting primary igneous features. A thick ( $\sim 1$  mm wide; 10.4 vol% abundance) vein of melt material transects the sample [6]. This feature is distinct from thin glassy networks of veins present elsewhere in NWA 4797 and in other shergottites (e.g., Zagami), but is similar to those larger ‘melt dikes’ described in ordinary chondrites [9] and in shergottite Y000027 [10].

Olivine shows a wide range of microtextures attributed to shock. Within both lithologies olivine exhibits strong mosaicism and pervasive fracturing. The fractures are irregular and open; no planar elements have been observed despite a systematic search of over 30 grains. In plane light olivine is pale brown and weakly pleochroic; however, in poikilitic regions olivine grain boundaries show evidence for partial melting and local recrystallization. These regions are colorless in plane transmitted light. In non-poikilitic regions olivine grains exhibit cusped and curved margins, a texture that is most pronounced in direct contact with the plagioclase melt. Trails and stringers of minute ( $< 1$  mm) iron sulfides are common, giving the grains a locally blackened appearance.

Pyroxene shows deformed, recrystallized and partially melted margins, a feature that is most pronounced in non-poikilitic regions, as also observed for olivine. The large pigeonite oikocrysts exhibit polysynthetic twinning associated with shock. The birefringence of pigeonite is reduced ( $\delta = 0.005\text{--}0.008$ ), while augite exhibits typical second order interference colors. Pyroxene grains in both lithologies exhibit strong mosaicism and are heavily fractured. One oikocryst contains a set of roughly parallel (but not straight) glass films from which open fractures nucleate.

Precursor igneous plagioclase in interstitial (non-poikilitic) regions has been completely melted, vesiculated, and mobilized throughout the host rock. Cooling of this melt has resulted in complex recrystallization textures and relationships with other minerals in both

lithologies. The margins between glass and adjacent minerals (olivine / chromite / pyroxene) are not sharp but have curved and cusped boundaries, with marked zoning (1–2  $\mu\text{m}$ ) in direct contact with the glass. Migration of the melt from interstitial regions occurs along grain boundaries or as stringers of melt (2–20  $\mu\text{m}$ ) cutting across neighboring minerals. These stringers extend into the poikilitic lithology and can be traced to distances  $\sim 600 \mu\text{m}$  indicating significant mobilization of melt. Varying contributions from olivine and pyroxene result in the presence of olivine and / or pyroxene crystallites in addition to the plagioclase microlites. With increased volumes of melting the textures progress from thin (1–20  $\mu\text{m}$ ) stringers of plagioclase glass to larger veins of melt containing olivine and plagioclase crystallites, and finally to unmolten olivine and pyroxene grains, and rock fragments pervasively invaded, and completely surrounded, by melt. At the melt dike margin, the plagioclase melt from interstitial regions and the melt-intruded regions intermingles with the groundmass of the melt dike.

**Composition:** Major mineral compositions and INAA data for NWA 4797 fusion crust have been reported by [6]. Given the small amount of sample available for scientific study and the relatively coarse grain-size, we have calculated the bulk composition using the mineral mode (obtained by 12,000 points) combined with electron microprobe analyses of constituent phases to be (wt%):  $\text{SiO}_2$  (41.6),  $\text{TiO}_2$  (0.4),  $\text{Al}_2\text{O}_3$  (3.7),  $\text{Cr}_2\text{O}_3$  (2.0),  $\text{FeO}$  (19.9),  $\text{MnO}$  (0.5),  $\text{MgO}$  (25.6),  $\text{CaO}$  (4.7),  $\text{Na}_2\text{O}$  (0.7),  $\text{K}_2\text{O}$  (0.1) and  $\text{P}_2\text{O}_5$  (0.4). We note that our calculated  $\text{FeO}$  and  $\text{Na}_2\text{O}$  values are within error to INAA values reported by [6].

**Discussion:** Comparisons between shock-induced effects in NWA 4797 olivine, pyroxene and plagioclase, and those observed in samples from calibrated shock recovery experiments [e.g., 9, 11, 12], have been used to constrain the equilibration shock pressure of NWA 4797. Shock-recovery experiments on dunite at 59 GPa [11] show intergranular melting and recrystallization at this pressure. Similar textures have also been reported from [12] for pressures of 60 GPa (293 K starting temperature). Planar elements in olivine are not observed above  $\sim 60$  GPa [9, 11, 12]. The reduced birefringence observed in pigeonite ( $\delta = 0.005\text{--}0.008$ ) develops above 50 GPa [9], whereas mechanical twinning begins at  $\sim 10$  GPa and persists over a wide range ( $< 80$  GPa; [9]). Shock effects in NWA 4797 thus indicate a minimum shock pressure of  $\sim 59\text{--}60$  GPa, corresponding to a post-shock temperature increase  $> 1000^\circ\text{C}$ . The upper pressure limit can be constrained to be less than that required for whole rock melting:  $\leq 75$  GPa. Based on the contact relationships, the plagioclase melts and vein-intruded

class melts and vein-intruded regions were produced in the same event that also formed the mm-size melt dike.

**Conclusions:** NWA 4797 is nearly identical in terms of the petrography of igneous lithologies, mineral compositions, modal abundance, oxygen fugacity and bulk composition to some “lherzolitic” shergottites; however, REE abundances [6] indicate that this meteorite may be derived from a distinct mantle source region. NWA 4797 is also distinguished by its strong degree of shock damage, representing a growing group of Martian meteorites shocked to pressures  $> 55$  GPa, previously represented only by Dhofar 378. Shock melts are locally derived, and therefore do not represent a source of extraneous REE. Despite the strong degree of shock damage in NWA 4797 it remains in the class of crystalline igneous rocks and is not a breccia. The shock effects observed in this study are associated with the strongest impact experienced by the rock; whether or not these effects are associated with Mars’ near-surface ejection or impact relocation on Mars and later ejection will be addressed by future Ar-Ar laser probe work.

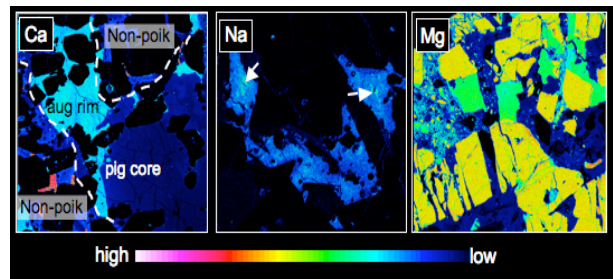


Fig. 1. Elemental X-ray maps showing the two igneous lithologies (Ca), interstitial recrystallized plagioclase (Na) in the non-poikilitic region, and a pervasively melt-veined region (Mg). The Na-rich cores of the recrystallized plagioclase (arrows) are also rich in  $\text{K}_2\text{O}$  (up to 3.8 wt%).

**References:** [1] Bogard and Johnson (1983) *Science*, 221, 651-654. [2] Fritz et al. (2005) *MAPS*, 40, 1393-1411. [3] Treiman (1998) *MAPS*, 33, 753-764. [4] Treiman et al. (2007) *JGR* 112, E04002. [5] Park et al. (2008) *JGR* 113, E08007. [6] Irving et al. (2008) *LPS XXXIX*, Abstract #7654. [7] Herd et al. (2002) *GCA*, 66, 2025-2036. [8] Goodrich et al. (2003) *MAPS*, 38, 1773-1792. [9] Stöffler et al. (1991) *GCA*, 55, 3845-3867. [10] Mickouchi T. and Kurihara T. (2007) *MAPS Suppl.*, Abstract #5290. [11] Reimold and Stöffler (1978) *Proc. 9<sup>th</sup> LPSC*, 2805-2824. [12] Schmitt (2000) *MAPS*, 35, 545-560.